RSC Advances

ROYAL SOCIETY
OF **CHEMISTRY**

www.rsc.org/advances

RSC Advances

RSCPublishing

PAPER

High Dielectric Constant and Low Loss of Polymeric Dielectric Composites Filled by Carbon Nanotubes Adhering BaTiO₃ Hybrid Particles

Z. D. Liu, [a] Y. Feng, [b] W. L. Li, [* b , c]

We reported the preparation of carbon nanotubes adhering BaTiO₃ nanoparticles (BT@CNTs) via chemical vapor deposition (CVD). The scanning electron microscope and Raman spectra were carried out in order to confirm the successful adhesion. Dielectric properties of the PVDF-HFP composites filled by BT@CNTs were also studied. With the content of BT@CNTs increasing, the dielectric constant of composites remarkably increased, but the loss tangent gradually decreased. At 10vol%, the dielectric constant of PVDF-HFP/BT@CNTs composite was significantly increased to 27.7 at 50 Hz, which was 3 times and 65% higher than that of the pure PVDF-HFP and PVDF-HFP/BT composite, respectively. The loss tangent of PVDF-HFP/BT@CNTs composite was lower even than that of pure PVDF-HFP. These attractive features of PVDF-HFP/BT@CNTs composites suggested that the method proposed herein was a new approach to develop high performance composites, especially those with high dielectric constant and low dielectric loss.

Introduction

In recent years, polymer composites with high dielectric constant have been paid much attention for their promising applications in capacitors, gate dielectrics actuators, energy storage and high-density electronic packaging technology, etc.[1-6] Specifically, capacitors with high dielectric constant and low dielectric loss are highly desired to meet the miniaturization requirement of the electronic devices and ensure good performance. To achieve better performance in these areas, many works have been focused on improving the dielectric properties of the materials by introducing various fillers into the polymer matrix.[7, 8, 9] The one of traditional ways is to develop percolative dielectric material with conductive particles as fillers. For the percolative polymer composites, various nano-sized metal particles including Ni, Al, and Ag have been employed as conductive fillers.[10-15] According to the percolation theory, the effective dielectric constant of the composites can be dramatically increased when the concentration of conductive fillers approaches percolation threshold. However, the tangent, and high conductivity make it difficult to acquire desired electrical property of the polymer-conductor composites. To reduce the conductivity and loss tangent of the percolative composites, researchers have performed an insulating interlayer or shell on the surface of

[a] China Lanzhou Institute of Physics, Lanzhou 73000, P.R. China.

[b] School of Materials Science and Engineering, Harbin Institute of Technology, Harbin 150001, P.R. China. Email: wlli@hit.edu.cn

[c] National Key Laboratory of Science and Technology on Precision Heat Processing of Metals, Harbin Institute of Technology, Harbin 150001, P.R. China.

conductive fillers to prevent the conductive particles from contacting with each other, or introducing ceramics to the conductor-polymer systems.[2, 16, 17] However, it is still hard to achieve a balance between high permittivity and low loss. Another way to improve the dielectric constant is to disperse some high-k ceramic powders into polymers to form 0–3 type composites. Ferroelectric ceramic powders with high dielectric constant, such as barium titanate (BT) and calcium copper titanate (CCTO), have also been chosen as fillers in order to acquire relatively high dielectric constant.[18-20] However, the largest disadvantage of ceramic/polymer based composites is that the high volume fraction (>50 vol%) of the filler is necessary to fabricate high-k composites, which may significantly deteriorate the flexibility of the polymer matrix. Because perfect interface between polymer and ceramic powder can enhance effectively interfacial polarization, many studies have been focused on the modification of the ceramics nanoparticles filler to increase the compatibility between ceramics and polymer matrix. The surface of ceramics is usually modified by surfactant adsorptions, polymer coatings or conductive materials coatings, and a physical compatibility along with more novel interface can be formed to guarantee good dispersion of the ceramics particles.[21-24] Recently, many researchers had reported that the nano-sized Ag particles discretely deposited on the BT surface can efficiently enhance the dielectric permittivity of the BT-Ag/PVDF composite. Theoretical calculations suggested that the enhanced permittivity of BT-Ag/PVDF composites should arise from the ultrahigh permittivity of BT-Ag fillers, which was over 10^4.[25] Lots of previous studies demonstrate that conductive materials coatings on the ceramic particles can result in enhanced dielectric properties in the polymer based composites.

In the present study, the fabrication of carbon nanotubes (CNTs) adhering $BaTiO_3$ nanoparticles and PVDF-HFP/BT@CNTs composites were investigated. The CNTs adhering $BaTiO_3$ nanoparticles were characterized by scanning electron microscope (SEM) and Raman spectra, and the composites were also studied by scanning electron microscope (SEM) and X-ray diffraction (XRD). In addition, the dielectric properties of the composites filled by the BT@CNTs and correlation with the structure and morphology of the composites are also discussed. The BT@CNTs in the composites was found to have significant and interesting influences on the dielectric properties of the composite system.

Experimental

Materials

PVDF-HFP was purchased from Sigma-Aldrich Co. Ltd. $BaTiO_3$ nanoparticles (BT-NPs) purchased from Aladdin Industrial Corporation with the size of 100nm were sieved out prior to use. Carbon nanotubes adhering $BaTiO_3$ hybrid particles (BT@CNTs) were fabricated by CVD, and the preparation process was shown in the Scheme 1. Nickel nitrate hexahydrate ($NiNO_3$ $6H_2O$) and methanol were purchased from Shanghai Chemical Corp. All chemicals are used without further purification. All other chemicals were obtained as analytical grade products and used without further purification.

Preparation of BT@CNTs

In this process, 3 g $Ni(NO_3)_2$ $6H_2O$ was dissolved into methyl alcohol. A 7 g BT was then added with fast stirring. The mixture was stirred vigorously for 60 min and then heated at 100 ℃ for 4 h to remove methanol, which was subsequently cooled to room temperature. The products were $BaTiO_3@Ni(NO_3)_2$ $6H_2O$. In order to adhere CNTs to the $BaTiO_3$ nanoparticles, the catalyst-coated $BaTiO_3$ nanoparticles were placed at the centre position of a quartz tube reactor heated to about 800 ℃ under flowing argon/hydrogen (10:1 molar ratio) gas mixture. After reaching to the desired temperature (800 ℃), a flow of methane (CH_4) gas was introduced into the reactor with a rate of 20 Sccm for about 30 min. A black coating covered the surface of the nanoparticles is CNTs. Then quartz tube reactor was subsequently cooled to room temperature. The black powder is BT@CNTs.

Scheme 1. Synthesis of BT@CNTs

Preparation of PVDF-HFP composites

The PVDF-HFP/BT@CNTs composites were prepared by employing solution blend. The BT@CNTs were ultrasonically dispersed in N,N-Dimethylformamide (DMF) for 0.5h. Then PVDF-HFP was added into the system with mechanical stir for 2h at 70 ℃. Then the mixture was casted on clean glass plates and dried at 120 ℃ for 2h in an oven. The prepared composites filled with various filler concentration and thickness of 25-35μm were collected for test.

Table 1. Technology parameters of BT@CNTs

	Pressure	Catalyst	Temperature	Gas	Time
CNTs	Ordinary pressure	Ni	800 ℃	CH_4/H_2-Ar 20/80	30 min

Characterization

The scanning electron microscope (SEM) observation was performed on a Helios Nanolab 600i. The transmission electron microscope observation was performed on a Tecnai F30. The wide-angle X-ray diffraction (XRD) experiment was performed on a Philips X'Pert diffractometer with CuKα radiation generated at 40kV and 40mA. Raman analysis was carried out using a micro-Raman Renishaw spectrometer. The laser line (514nm) was used to excite the sample. The broadband dielectric spectroscopy was carried out using a Agilent 4294. Prior to dielectric measurements, the relative humidity (≈50%) of the measurement environment remain constant throughout the investigation.

Results and Discussions

Characterization of BT@CNTs and Composites

Raman spectra can be used to reveal the graphitic nature of the fabricated CNTs. Fig. 1 shows the Raman spectra of the BT@CNTs powder. The peak at 1574 cm^{-1} is a so-called G-band, and those at 1321cm^{-1} are D-band. The G-band comes from the stretching of conjugated double bonds corresponding to sp^2 hybridization during the formation of the arylnanotube bond, and the D-band is associated with vibrations of carbon atoms with dangling bonds in plane terminations of the disordered graphite or glassy Carbons. The intensity ratio of I_D/I_G is known to depend on the structural characteristics of CNTs, and is a usual measurement of the graphitic ordering. The I_D/I_G value of the spectrum suggests a defective structure or a lower degree of graphitization in CNTs structure. In the Fig. 1, the I_D/I_G value of the spectrum is about 0.8, which demonstrates that higher quantity CNTs are adhered on BT nanoparticles.
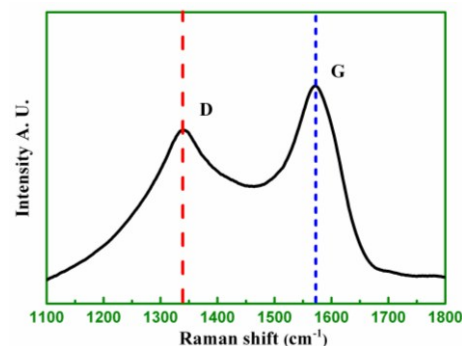

Figure 1 Raman spectra of BT@CNTs

The SEM and TEM images of as-synthesized BT@CNTs hybrid particles are shown in Fig. 2. As shown in Fig. 2(a) and

(b), it is clear that the CNTs with a diameter of 30-70 nm are dispersed on the BT surface. The Fig. 2(b) displays a image of BT@CNTs with higher magnification, which clearly shows that one side of the CNTs is in connect with the BT particles. In order to further confirm the adhesion, TEM image of BT@CNTs and high resolution TEM image of interfacial microstructures are displayed in the Fig. 2(c) and (d), respectively. The observation in Fig. 2(c) is consistent with that in Fig. 2(b), which indicates that the CNTs are adhered on the surface of BT. Fig. 2(d) confirms that the combination between BT and CNTs is strong, and no phase separation exists.
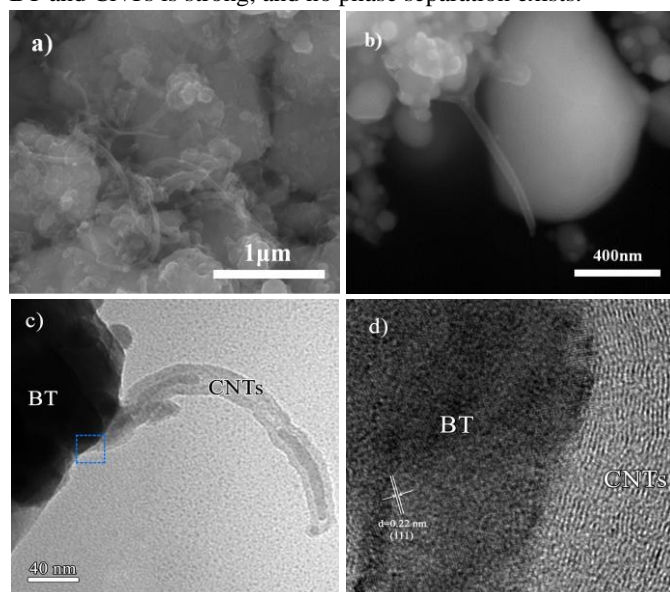

Figure 2 SEM images (a and b) and TEM images (c and d) of BT@CNTs, (d) is the high resolution TEM image in the dashed line square of (c)

Fig. 3 shows the XRD patterns of pure PVDF-HFP and PVDF-HFP/BT@CNTs composite. The peaks at 18.4°, 20.8° and 26.6° correspond to the PVDF α-phase, β-phase and γ-phase diffraction, respectively. For the composite, the characteristic diffraction peaks of $BaTiO_3$ appear at about 2θ =22°, 31°, 38°, which are associated with typical structure of perovskite $BaTiO_3$ in crystal planes of (100), (110) and (111). Because the characteristic of CNTs in XRD pattern is not obvious, there is no peak corresponding to CNTs. After BT@CNTs were incorporated into the PVDF-HFP matrix, the XRD pattern of the composite shows both $BaTiO_3$ and PVDF-HFP diffraction peaks, which clearly demonstrates that BT@CNTs are filled in the polymer matrix.
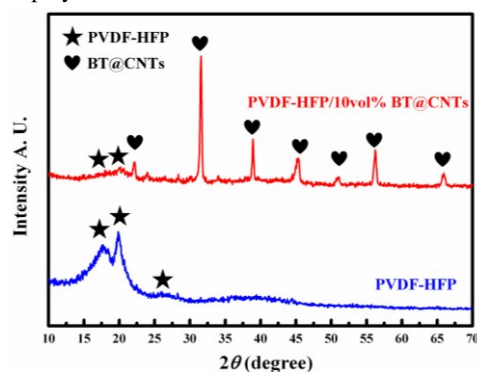

Figure 3 XRD patterns of PVDF-HFP and PVDF-HFP/BT@CNTs composite

In order to research the effect of hybrid filler on the dielectric properties of composites, we fabricated two kinds of composites containing BT@CNTs and BT filler, respectively. Fig. 4 displays cross section SEM images of PVDF-HFP/BT and PVDF-HFP/BT@CNTs composites. BT particles with sphere disperse homogeneously into the PVDF-HFP matrix. Moreover, the dispersion of BT@CNTs in the matrix is excellent. There are some wire-like fillers found (dashed lines) in the matrix, which should be the CNTs.
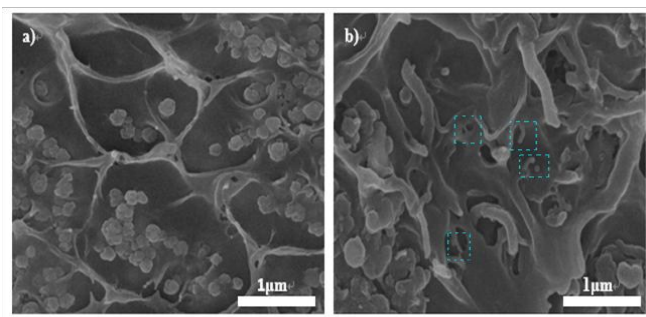

Figure 4 Cross section SEM images of (a) PVDF-HFP/10vol%BT, (b) PVDF-HFP/10vol% BT@CNTs composite

Dielectric properties of composites

The dependence of the dielectric constant of composites on the frequency is shown in Fig. 5. With the frequency increasing, the dielectric constants of two composites both decrease, because the different types of polarizations will not keep up with the variation of the AC frequency and gradually vanish one by one. With BT@CNTs content increasing, the dielectric constant of the composites increases. As the ceramic fillers have a much larger permittivity, most of the increase in effective dielectric constant of the composites comes from the increase in the average field in the polymer matrix. Compared with the composites filled by BT, it is clearly demonstrated that the dielectric constant of the composite can be significantly improved by filling BT@CNTs.
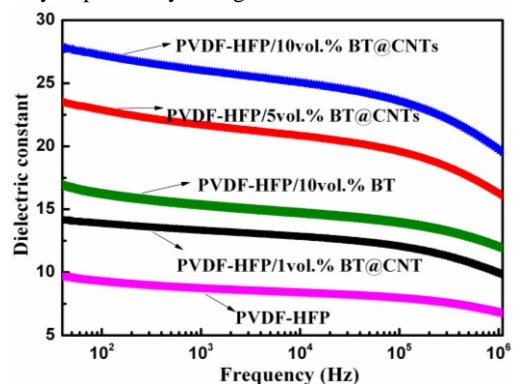

Figure 5 Dependence of dielectric constant of PVDF-HFP/BT@CNTs composites on the frequency at room temperature

The Fig. 6 shows loss tangent as a function of frequency for PVDF-HFP/BT@CNTs composites. With the frequency increasing, the loss tangent of composites decreases firstly, then increases. The loss tangent of PVDF matrix is around 0.065 at 50 Hz. The values of PVDF-HFP/1vol%BT@CNTs, PVDF-HFP/5vol% BT@CNTs and PVDF-HFP/10vol%BT@CNTs are 0.035, 0.05 and 0.043, respectively. In addition, the corresponding loss tangent of

composite with 10vol%BT is 0.072, higher than that of PVDF-HFP and PVDF-HFP/BT@CNTs composites. The results demonstrate that the BT@CNTs rather than BT can not only enhance the dielectric constant, but also reduce the loss tangent.
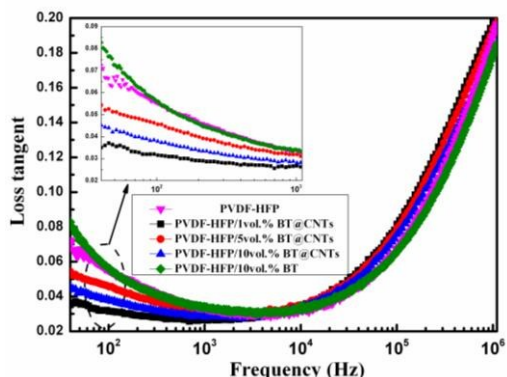

Figure 6 Dependence of dielectric loss of PVDF-HFP/BT and PVDF-HFP/BT@CNTs composites with different filler contents on the frequency at room temperature

Fig. 7 shows dielectric constant and loss tangent of the composites measured at 50 Hz as a function of volume fraction BT@CNTs. It should be noted that the dielectric constant of the composites increases with content of BT@CNTs increasing. Interestingly, the loss tangent has a downtrend when the BT@CNTs are incorporated into matrix. Evidently, the trend is not consistent with percolation theory, which is always used to explain many dielectric phenomena in the composites filled by CNTs.
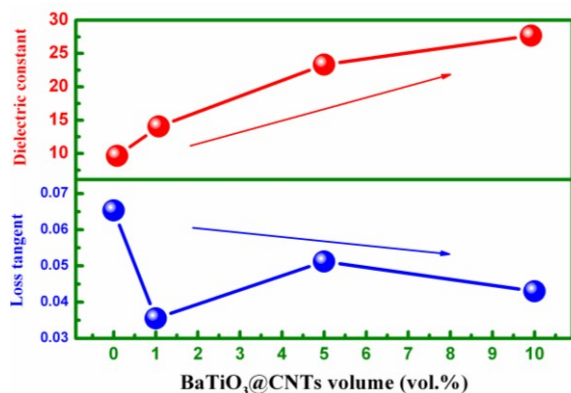

Figure 7.Dielectric constant and loss tangent of the composites measured at 50Hz as a function of volume fraction BT@CNTs

The Fig. 8 shows the dielectric constant and loss tangent of PVDF-HFP, PVDF-HFP/10vol%BT@CNTs and PVDF-HFP/10vol% BT composites. Among samples above, the dielectric properties of PVDF-HFP/BT@CNTs composite are outstanding because of its highest dielectric constant and lowest loss tangent. For the PVDF-HFP/10vol% BT@CNTs composite, the dielectric constant is about 27.7 at 50 Hz. And yet, the values of PVDF-HFP and PVDF-HFP/10vol% BT composite are only about 9.6 and 16.7, respectively. It should be noted that the dielectric constant of the composite with 10vol% BT@CNTs is 65% higher than the sample with 10vol% BT and 3 times larger than the polymer matrix. In the light of these dielectric features, it can be concluded that the increase in dielectric constant of PVDF-HFP/BT@CNTs composite is

attributed to the combination of BT and CNTs. The CNTs, as a kind of conductive filler own high aspect ratio and have a function to enhance dielectric constant effectively. Besides, the interfacial polarization, which normally exists between polymer and conductive fillers give rise to a much increased dielectric constant. However, the downtrend of loss tangent does not agree with some classical theory, for example Maxwell-Wagner and percolation theory. First of all, the content of CNTs on the BT is much low, which is far from percolation threshold of CNTs in the polymer. Secondly, one side of CNTs is connected with insulting BT particles, which efficiently prevents the continuous contact among CNTs in the matrix and suppresses the formation of the conducting path in the composite. With the CNTs adhering to the BT, the miscibility of filler and polymer matrix should be improved. In addition, the length and diameter of CNTs is small, in the range of 0.5-1μm and 30-70nm, respectively. A type of conductive filler with such small size possibly induces Coulomb blockade effect into polymer matrix. The size of CNTs conforms to requirement of "Coulomb Island".[7, 26] The tunnelling electron creates an additional barrier due to the charging energy $e^2/2C$ (where e is the electron charge unit, and C is the capacitance of the Coulomb island) to inhibit the further transfer of electrons. When the charging energy exceeds the thermal fluctuation energy k_BT (where k_B is the Boltzman constant, and T is the absolute temperature), the Coulomb blockade will occur, which inhibits the charge transfer through the small island below a certain voltage threshold and leads to an increase in resistance. Thus, the loss tangent of PVDF-HFP/BT@CNTs is lower than that of PVDF-HFP and PVDF-HFP/BT composite.
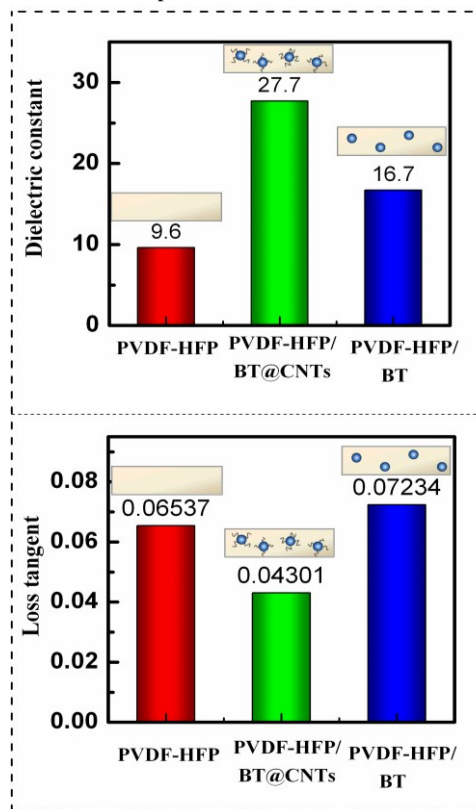

Figure 8.Comparasion of dielectric constant and loss tangent at 50 Hz between PVDF-HFP, PVDF-HFP/BT@CNTs and PVDF-HFP/BT composites

Conclusions

1. The BT@CNTs were fabricated by adhering CNTs to the suface of BT nanoparticles via CVD.

2. The high dielectric constant PVDF-HFP/BT@CNTs composites were prepared via casting method. For the PVDF-HFP/10vol% BT@CNTs composite, the dielectric constant is about 27.7 at 50 Hz, which is 65% higher than the composite with 10 vol% BT and 3 times larger than the polymer matrix.

3. Compared with PVDF-HFP and PVDF-HFP/BT composite, the loss tangent of PVDF-HFP/BT@CNTs is lowest, which may be due to the Coulomb blockade effect of CNTs on the surface of BT nanoparticles.

Acknowledgements

Notes and references

1. L. Gao, J. L. He, J. Hu and Y. Li, *J Phys Chem C*, 2014, **118**, 831-838.
2. T. Lei, Q. Z. Xue, L. Y. Chu, Z. D. Han, J. Sun, F. J. Xia, Z. Y. Zhang and Q. K. Guo, *Appl Phys Lett*, 2013, **103**.
3. Y. Deng, Y. J. Zhang, Y. Xiang, G. S. Wang and H. B. Xu, *J Mater Chem*, 2009, **19**, 2058-2061.
4. B. C. Luo, X. H. Wang, Y. P. Wang and L. T. Li, *J Mater Chem A*, 2014, **2**, 510-519.
5. Y. Feng, W. L. Li, Y. F. Hou, Y. Yu, W. P. Cao, T. D. Zhang and W. D. Fei, *J Mater Chem C*, 2015, **3**, 1250-1260.
6. X. W. Liang, S. H. Yu, R. Sun, S. B. Luo, J. Wan, S. H. Yu, R. Sun, S. B. Luo, X. W. Liang, J. Wan and Z. Q. Zhuang, *J Mater Res*, 2012, **27**, 991-998.
7. J. X. Lu, K. S. Moon, J. W. Xu and C. P. Wong, *J Mater Chem*, 2006, **16**, 1543-1548.
8. N. Yousefi, X. Y. Sun, X. Y. Lin, X. Shen, J. J. Jia, B. Zhang, B. Z. Tang, M. S. Chan and J. K. Kim, *Adv Mater*, 2014, **26**, 5480-5487.
9. S. H. Kim, M. Jang, J. Kim, H. Choi, K. Y. Baek, C. E. Park and H. Yang, *J Mater Chem*, 2012, **22**, 19940-19947.
10. Y. Deng, Y. J. Zhang and Y. Z. Song, *Rare Metal Mat Eng*, 2009, **38**, 583-585.
11. W. Y. Zhou, J. Zuo and W. N. Ren, *Compos Part a-Appl S*, 2012, **43**, 658-664.
12. M. Panda, V. Adyam, V. Srinivas and A. K. Thakur, *Aip Conf Proc*, 2008, **1003**, 43-45.
13. A. Kono, K. Shimizu, H. Nakano, Y. Goto, Y. Kobayashi, T. Ougizawa and H. Horibe, *Polymer*, 2012, **53**, 1760-1764.
14. X. W. Kuang, Z. Liu and H. Zhu, *J Appl Polym Sci*, 2013, **129**, 3411-3416.
15. L. Zhang, D. Q. Xiao and J. Ma, *Ferroelectrics*, 2013, **455**, 77-82.
16. W. Cui, F. P. Du, J. C. Zhao, W. Zhang, Y. K. Yang, X. L. Xie and Y. W. Mai, *Carbon*, 2011, **49**, 495-500.
17. T. Zhou, J. W. Zha, Y. Hou, D. Wang, J. Zhao and Z. M. Dang, *Acs Appl Mater Inter*, 2011, **3**, 4557-4560.
18. Y. Feng, J. H. Yin, M. H. Chen, M. X. Song, B. Su and Q. Q. Lei, *Mater Lett*, 2013, **96**, 113-116.
19. Z. M. Dang, T. Zhou, S. H. Yao, J. K. Yuan, J. W. Zha, H. T. Song, J. Y. Li, Q. Chen, W. T. Yang and J. Bai, *Adv Mater*, 2009, **21**, 2077-2082.
20. Y. Song, Y. Shen, H. Liu, Y. Lin, M. Li and C. W. Nan, *J Mater Chem*, 2012, **22**, 8063–8068.
21. D. R. Wang, T. Zhou, J. W. Zha, J. Zhao, C. Y. Shi and Z. M. Dang, *J Mater Chem A*, 2013, **1**, 6162-6168.
22. T. Zhou, J. W. Zha, R. Y. Cui, B. H. Fan, J. K. Yuan and Z. M. Dang, *Acs Appl Mater Inter*, 2011, **3**, 2184-2188.
23. L. Y. Xie, X. Y. Huang, Y. H. Huang, K. Yang and P. K. Jiang, *Acs Appl Mater Inter*, 2013, **5**, 1747-1756.
24. X. Zhang, Y. Ma, C. Zhao and W. Yang, *Appl Surf Sci*, 2014, **305**, 531-538.
25. S. Luo, S. Yu, R. Sun and C. P. Wong, *Acs Appl Mater Inter*, 2014, **6**, 176-182.
26. Q. Q. Feng, Z. M. Dang, N. Li and X. L. Cao, *Mat Sci Eng B-Solid*, 2003, **99**, 325-328.